JOURNAL OF Materials CHEMISTRY

Nanocrystalline LiF *via* microemulsion systems

Marcel Roth and Rolf Hempelmann*

Physikalische Chemie, Universität des Saarlandes, 66123 Saarbrücken, Germany

Received 18th September 1998, Accepted 16th November 1998

LiF has been prepared in nanocrystalline form by means of microemulsion-mediated precipitation of NH_4F and LiOAc. Grain growth during the intermicellar exchange, *i.e.* Ostwald ripening due to the comparatively high solubility of LiF, was suppressed by a strict control of the reaction time. For short times a flowmixer with a certain tube length was used. The reaction was stopped by coagulation in acetone. On heating, the by-product, NH_4OAc, transforms into acetamide which can easily be extracted. The resulting nano-LiF was isolated as a powder; it exhibits grain sizes between 25 and 70 nm, depending on the reaction time.

1 Introduction

Preparation of monodisperse, ultrafine particles is one of the important goals in modern chemical engineering, *e.g.*, in catalysis, ceramic processing, solar energy conversion processes, as well as in pharmaceutical and photographic technology. Such a preparation with size-control can be peformed in water-in-oil microemulsions which have already successfully been used for this purpose.[1,2] In contrast to macroemulsions, microemulsions are optically transparent, isotropic, thermodynamically stable dispersions of oil in water (o/w-microemulsions) or water in oil (w/o-microemulsions). They form spontaneously by mixing a hydrophobic and a hydrophilic solvent with an emulsifing agent in well defined proportions. In the case of water-in-oil microemulsions the surfactant and the water form reverse micelles which can be employed as so-called nano-reactors. Starting from two w/o-microemulsion systems loaded with appropriate aqueous salt solutions, it is possible to precipitate nanosize crystals simply by mixing the microemulsions. This is a consequence of the intermicellar exchange of the salt solutions contained in the aqueous cores of the micelles.

A review of nano-particles and nano-precipitates in microemulsions is given by Osseo-Asare and Arriagada.[3] The solubility of precipitates produced up to now (*e.g.*, nano-CdS, nano-PbS, nano-AgCl, nano-Fe_3O_4) is $<10^{-5}$ mol (kg $H_2O)^{-1}$. In the case of more soluble precipitates severe difficulties arise such as fast agglomeration and low yields; in addition it is a problem to find a microemulsion system which is able to stabilise highly concentrated salt solutions without salting out.[4]

In many synthesis routes the precipitation is initiated by bubbling a gas (CO_2, NH_3, H_2S) through *one* microemulsion. But to the best of our knowledge only nano-AgCl,[5] nano-$CaSO_4$[6] and nano-NH_4MnF_3[7] have been synthesised up to now *via* mixing of *two* microemulsions each containing the aqueous solution of a salt. The main problem of the latter syntheses is the isolation of a chemically pure powder which was not possible in the case of nano-AgCl[5] and nano-$CaSO_4$.[6] Recently, however, we succeeded in preparing appreciable amounts of nano-NH_4MnF_3,[7] a salt with a solubility at room temperature of 0.115 mol (kg $H_2O)^{-1}$.[8]

In the present contribution we improve our preparation route and extend it to another relatively soluble salt, *i.e.* to LiF, with a solubility at room temperature of 0.0513 mol (kg $H_2O)^{-1}$.[9] The substance is chemically inert and not hygroscopic. The simple cubic crystal structure (NaCl-type)[10] means that LiF is an ideal system for investigations of, *e.g.*, the optical properties of nanostructured materials.[11]

2 Experimental

2.1 Chemicals

All chemicals were of the best quality commercially available, and were used without further purification: AOT-sodium salt, AOT = bis(2-ethylhexyl) sulfosuccinate, (Fluka), *n*-heptane (Fluka), $LiCH_3CO_2$ (Fluka), NH_4F (Fluka), acetone (Merck). The water was ion-exchanged and active-coal filtered.

2.2 Microemulsion

Our microemulsion systems are based on *n*-heptane/AOT-NH_4, weight ratio 1.2. The conversion of the commercially available AOT-sodium salt into other salts is described by Kitahara[12] and Pileni and co-workers.[13] It can be performed by the metathesis reaction of methanolic AOT-Na and aqueous NH_4Cl solution or by ion-exchangers. After the conversion, the sodium content is $<10^{-4}$ wt%, as determined by flame spectroscopy.[7]

For materials chemistry in microemulsions it is essential to know their existence range. Therefore the relevant two-dimensional section of the phase diagram of the ternary system *n*-heptane–AOT-NH_4–aqueous NH_4F was determined at room temperature by the dropwise addition of differently concentrated salt solutions to mixtures of *n*-heptane/AOT-NH_4, weight ratio 1.2, under stirring: a water-clear appearance for several days indicated a stable microemulsion. Fig. 1 shows the result: the gray field indicates the range of stable micro-

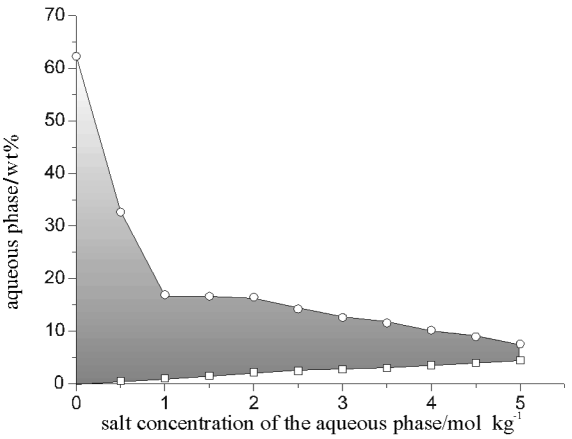

Fig. 1 The two dimensional phase diagram of the system *n*-heptane/AOT-NH_4 (w/w = 1.2) and aqueous NH_4F solutions at room temperature; the gray field indicates the range of stable microemulsions.

emulsions. The higher the concentration of the salt solution, the more solution is necessary to form a stable microemulsion and the less salt-solution can be stabilized. Microemulsions can still be formed even when the concentration exceeds 5 mol NH_4F (kg H_2O)$^{-1}$.

2.3 Synthesis

Choosing concentrations of LiOAc-solutions in suitable stoichiometry to the NH_4F solutions, the aqueous salt solutions are added to mixtures of *n*-heptane/AOT. These two mixtures are stirred, until a water-clear appearance and long-time stability indicate the formation of the two microemulsions.

Then these two microemulsions are mixed at room temperature under vigorous stirring. Although precipitation takes place, the reaction medium remains optically transparent because the nano-particles are colloidally stabilised. After a given time the precipitation reaction is stopped by pouring the sol into acetone under stirring (600 ml acetone per 100 ml sol). This results in the destruction of the microemulsion and the coagulation of the product powder. Simultaneously, in this step the by-product NH_4OAc is formed. The resulting raw powder, consisting of LiF and residual NH_4OAc, is purified by boiling it repeatedly in acetone followed by Soxhlet extraction (5 h). In this step NH_4OAc transforms into acetamide which dissolves in organic solvents. Finally, the raw product is calcined at 250 °C for 2 h to eliminate AOT adsorbed on the surface. X-Ray diffraction performed before and after calcination did not indicate any measurable crystal growth during this last step.

In order to realise very short but nevertheless well defined reaction times $\Delta t_{M\text{-}C}$ (for the preparation of the samples V and VI) the flowmixer shown in Fig. 2 was used (see Table 1, samples V and VI). The two microemulsions (A) containing the LiOAc and the NH_4F solution, respectively, were pumped by means of a double channel HPLC pump (B) (the advantage of this type of pump is that only stainless steel parts are in contact with the reaction medium) into a mixing chamber (C) where the two solutions are quickly mixed and the precipitation reaction starts. The process of precipitation and crystal growth proceeds while the mixture is flowing through the spiral Teflon flow-tube (D). In the whole flow-tube the reaction medium remains optically clear, *i.e.*, the reaction progress is invisible because the primary precipitated particles are much smaller than the wavelength of visible light. The flow-tube ends in stirred acetone (E) which dissolves the water and the surfactant and thus stops the reaction immediately; the raw product coagulates and is now visible as a precipitate. The flow velocity of the mixture was 27 ml min^{-1}. The diameter of the Teflon-tube was 1.5 mm and the length 3 m. This resulted in a reaction time of 12 s.

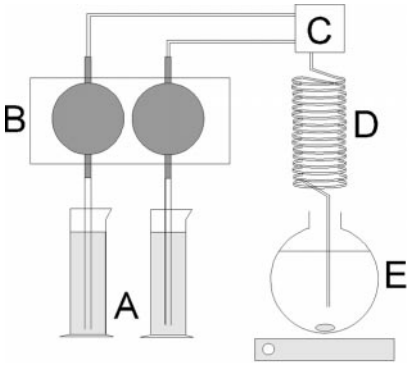

Fig. 2 Flow tube reactor for the realisation of short reaction times. Teflon, chemically inert towards organic solvents, is used as the tube-material. A detailed explanation is given in the text.

To avoid the formation of the possible by-product LiOAc, a slight excess of NH_4F was used. The concentration of the aqueous solution of NH_4F was 5.2 mol (kg H_2O)$^{-1}$ whereas the LiOAc concentration was chosen corresponding to a NH_4F concentration of 5.0 mol (kg H_2O)$^{-1}$. So, at any given time, the NH_4F concentration is kept higher than that of LiOAc. Uncertainties in the flow velocities caused by the pump can thus be tolerated. In contrast to LiOAc the resulting NH_4F impurities can easily be removed by sublimation in the calcination step.

2.4 Characterization

TEM micrographs were recorded using a JEOL 200CX transmission electron microscope; the sample-holder was a carbon net which had been drawn through a dispersion containing the powder; drying of the net was done at ambient temperature in the atmosphere.

Powder X-ray diffractograms were recorded at room temperature using a Siemens D 500 diffractometer with a flat hollowed plastic sample holder. Radiation was secondarily monochromated Cu-Kα, the sampling conditions were a scan in steps of 0.02° (2θ) with a step time of 2 s. The resulting diffraction pattern was compared with the JCPDS file system. From the broadening of X-ray diffraction peaks or, more precisely, from the line shape of these peaks the crystallite size can be determined. A common procedure is the Warren–Averbach method[14] which we use in a user-friendly modified version.[15,16] The resulting size distribution is described by the log-normal distribution function,

$$g(D)=\frac{1}{\sqrt{2\pi}\,D\,\ln\,\sigma}\exp\left[\frac{-(\ln\,D-\ln\,D_0)^2}{2(\ln\,\sigma)^2}\right]$$

with median diameter D_0 and the relative width σ.

3 Results

Our samples and the conditions of their syntheses are listed in Table 1. The parameters which mainly control the synthesis are (i) the reaction time $\Delta t_{M\text{-}C}$, *i.e.* the period of time between the mixing of the microemulsions and the coagulation with acetone and (ii) the content of the aqueous phase.

Other than for our nano-NH_4MnF_3 synthesis[7] the influence of the synthesis temperature was not studied because it turned out to have only a minor effect on the crystallite size. Furthermore the salt content was not systematically varied because the low mass yield, due to the low molecular weight (25.94 g mol^{-1}) of LiF, led us to use the highest possible salt concentrations which the microemulsion system was able to stabilise.

Fig. 3 shows the XRD pattern of a nanocrystalline LiF sample with the line broadening induced by the reduced size of the crystallites. TEM micrographs of samples II and III are shown in Fig. 4. TEM (a) (enlargement ×10 000) and (b) (enlargement ×50 000) show that all the crystallites of sample II are agglomerated into spheres. A difference in $\Delta t_{M\text{-}C}$ of 2 min (sample III *cf.* sample II) effects the transformation of the spheric agglomerates into cubic shaped agglomerates [see

Table 1 Synthesis parameters of nano-LiF prepared by microemulsion-mediated precipitation

Sample	[NH_4F]/mol (kg H_2O)$^{-1}$	$\Delta t_{M\text{-}C}$/ min	Weight% of aqueous phase
I	3.0	1	10
II	3.0	3	10
III	3.0	5	10
IV	3.0	1	5
V	5.2	0.2	5
VI	5.2	0.2	5

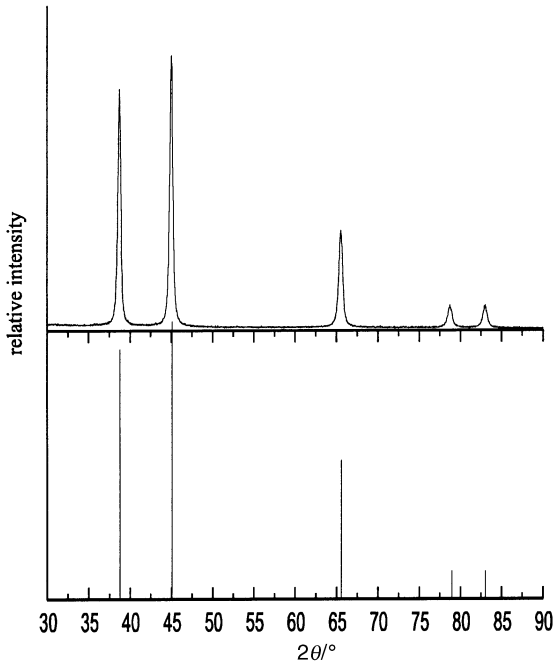

Fig. 3 XRD pattern of nano-LiF; upper part: experimental diffractogram, lower part: diffraction peaks of LiF according to the JCPDS file.

TEM (c) of sample III]. A comparison between the crystallite size distribution, determined by Warren–Averbach analysis, and the agglomerate-size distribution, determined by counting and measuring the diameter of more than 500 agglomerates, is given in Fig. 5.

Results of the size-controlling experiments are given in Table 2 and illustrated by the crystallite size distributions of the samples II, IV and VI shown in Fig. 6. The size distribution of sample III was not determined because the TEM micrograph [TEM (c) in Fig. 4] shows that the crystal diameters are not distributed according to a log-normal distribution. A comparison between the XRD pattern of calcined and uncalcined powders showed that no crystal growth occurred during calcination.

A longer reaction time $\Delta t_{\text{M-C}}$ leads to an increase of the crystallite size and a wider crystallite size distribution in the case of the samples I, II and III. The TEM images in Fig. 4 illustrate the crystal growth in the agglomerates with time. A shorter reaction time $\Delta t_{\text{M-C}}$ and a higher salt concentration used to prepare sample V did not lead to smaller crystallites.

A lower content of the aqueous phase (sample IV *cf.* sample I) effects a narrower grain size distribution and thus a decrease of the volume averaged crystallite size D_{V}. However, the maxima of the two crystallite size distributions (samples I and IV) are identical.

The smallest crystallites with the narrowest size-distribution which we have been able to produce were those of sample VI. The difference in the preparation of samples V and VI is only that in the case of sample VI *n*-heptane instead of acetone was used in the Soxhlet extraction. Obviously, other than for nano-NH_4MnF_3 the purification route seems to influence the resulting crystallite size and distribution of the LiF crystals.

Table 2 Crystallite size distribution of the resulting nano-LiF samples as determined by means of X-ray line shape analysis; D_0 and σ are the median diameter and the relative widths, respectively, of the log-normal distribution function, $<D_{\text{vol}}>$ is the volume averaged diameter

Sample	D_{o}/nm	σ	$<D_{\text{vol}}>$	Maximum of distribution/nm
I	19.1	1.58	40	15
II	22.0	1.49	39	19
III	—	—	69	—
IV	17.9	1.46	29	15
V	16.8	1.53	32	14
VI	14.27	1.51	25	12

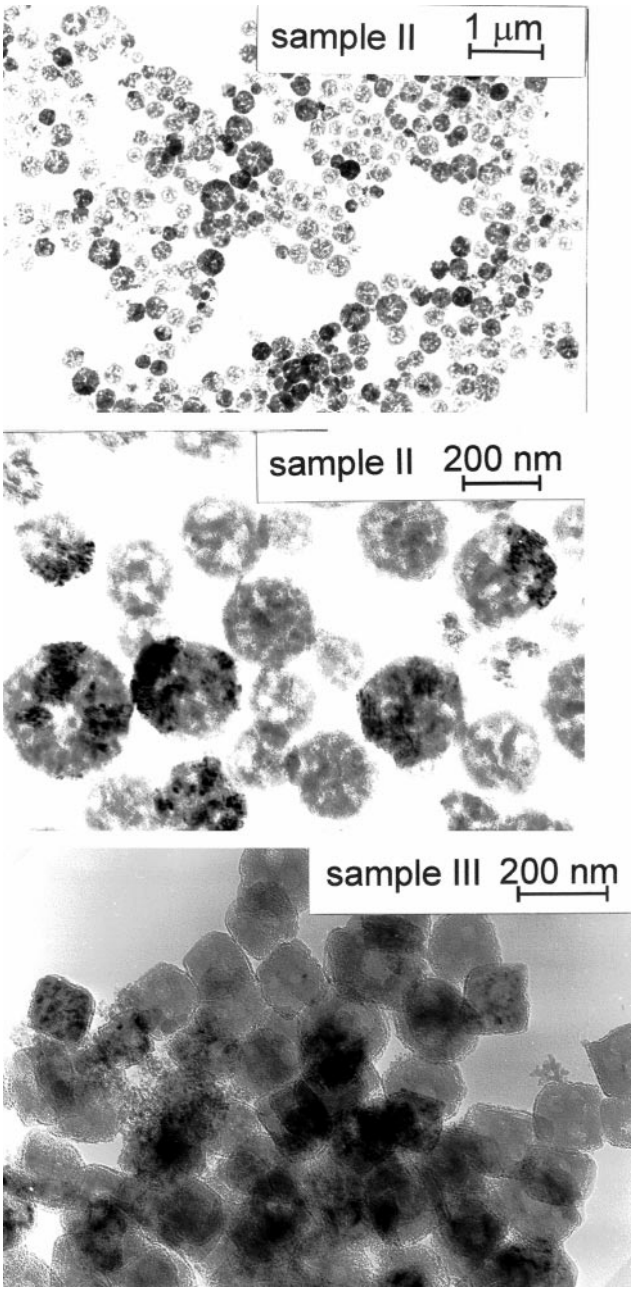

Fig. 4 TEM-micrographs of nano-LiF samples prepared in microemulsions. Sample II ($\Delta t_{\text{M-C}} = 3$ min, $D_{\text{V}} = 39$ nm): all the crystallites exist in the form of spherical agglomerates. Sample III ($\Delta t_{\text{M-C}} = 5$ min, $D_{\text{V}} = 69$ nm): the spherical agglomerates have transformed into cubic-like agglomerates. The micrograph of sample I is very similar to that of sample II and is therefore not displayed.

Polycrystalline LiF has an extremely low solubility in acetone (3.3×10^{-6} mol kg^{-1}).[14] It cannot, however, be excluded that the solubility of nano-LiF is higher such that Ostwald ripening could become appreciable. To investigate a possible crystal growth of the nanocrystalline LiF, sample IV was boiled in acetone for five days. After the evaporation of the solvent the crystallite size of the powder was determined by X-ray line shape analysis. However, no significant crystal-growth of the nano-powder of sample IV boiled in acetone was observed. The volume averaged crystallite diameter of the salt treated in this way was 31 nm compared with an initial value, D_{V}, of 29 nm.

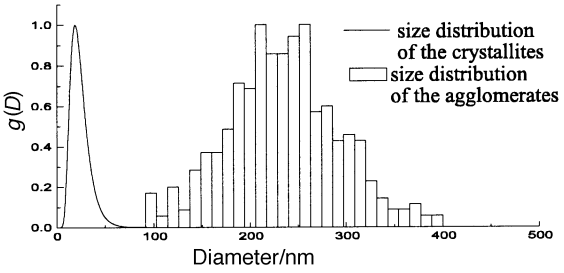

Fig. 5 The crystallite-size distribution and the size distribution of the agglomerates of sample II.

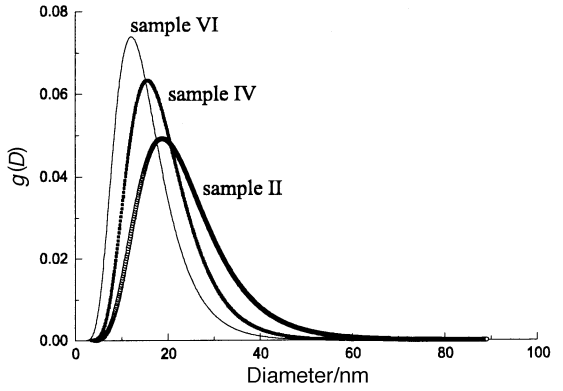

Fig. 6 Size distributions of the nano-LiF samples II, IV and VI.

The relative yield varied between 10 and 50%, corresponding to an absolute yield of 0.07–0.35 g per 200 g of microemulsion mixture. With respect to mass this is a very low value, but with respect to the number of moles it is not so poor owing to the low molar mass of LiF.

4 Discussion

As in the case of the nano-NH_4MnF_3 synthesis[5] the reaction time $\Delta t_{M\text{-}C}$, *i.e.* the time between mixing and coagulation, is one of the two synthesis parameters which has a decisive influence on the resulting crystallite sizes (the other being the water content as explained below). The fast growth processes of nanocrystals synthesised in microemulsion were not observed in other work.[17–19] Hou and Shah, for instance, studied the kinetics of the agglomeration of nano-AgCl sols[21] and found that within 250 min the particles grow only by a few nanometers, whereas we observe a growth orders of magnitude faster. As the solubilities of precipitates produced up to now *via* microemulsions are lower than those of NH_4MnF_3 [0.115 mol (kg $H_2O)^{-1}$] and LiF [0.051 mol (kg $H_2O)^{-1}$], it seems justified to assign the fast crystal growth to the relatively high solubilities of the two salts, which enables Ostwald ripening and coalescence to occur. This is impressively illustrated by the TEM micrographs shown in Fig. 4. In a time period of only 2 min spherical agglomerates of the nanocrystals transform into cubic-like agglomerates, and simultaneously the crystallites grow. Because of its residual solubility in water as well as acetone, LiF is certainly not a model system for microemulsion-provided precipitations; it is our purpose, however, to demonstrate that the technique works even in more difficult situations, although with less precision.

The influence of the content of the aqueous phase was not as significant as in the case of nano-NH_4MnF_3. The reduction of the aqueous phase content effects a decrease of the total volume of the water charged micelles (*i.e.* the sum of the volumes of all micelles contained in the microemulsion system); we suppose that the consequence is a smaller intermicellar exchange rate during the precipitation time and thus a smaller probability for the resulting particles to come into contact with each other, so that the agglomeration and growth processes are slowed down.

Other than for our nano-NH_4MnF_3 synthesis[7] the crystallite size distributions are not so clearly separated. One reason might be a fast agglomeration process in connection with crystal growth based on Ostwald ripening and coalescence. All the nano-LiF particles are agglomerated (see Fig. 4) whereas the particles of nano-NH_4MnF_3 investigated by TEM were only partially agglomerated.[7]

Unfortunately, the relative yield of the synthesis of nano-LiF is rather low, whereas for nano-NH_4MnF_3 it was 100%.[7] A possible explanation could be a higher solubility of the nanoparticles compared with the polycrystalline material in acetone, although this could not be proved.

However, a conceivable reason is the exchange of the Li^+ ions in the aqueous cores of the micelles for the NH_4^+-ions of the surfactant according to

$$\text{AOT-NH}_4 + \text{Li}^+ \rightleftharpoons \text{AOT-Li} + \text{NH}_4^+$$

Upon binding to the surfactant, Li^+ would no longer be completely available for the precipitation reaction. For example Nagy *et al.*,[22] by means of ^{13}C NMR spectroscopy, demonstrated that Ni(II) or Co(II) ions interact with hexanol molecules and are retained close to the surfactant/water interface in the cetyltrimethylammonium bromide/hexanol/water system, whereas this is not so for Fe(III) which is strongly hydrated and thus homogenously distributed in the interior of the water droplets of the reverse micelles, far from the interface.

In summary, LiF is the second relatively soluble salt which has been successfully isolated as a nano-powder from a microemulsion system in appreciable amounts and which could be characterized by X-ray diffractograms. By variation of the synthesis parameters samples with different mean crystallite sizes were prepared.

Acknowledgements

The work has been performed within the framework of Sonderforschungsbereich 277 Grenzflächenbestimmte Materialien at the University of Saarbrücken, and we gratefully acknowledge financial support by the Deutsche Forschungsgemeinschaft. R.H. thanks the Fonds der Chemischen Industrie for generous financial support.

References

1 H. Herrig and R. Hempelmann, *Mater. Lett.*, 1996, **27**, 287.
2 Ch. Beck, W. Härtl and R. Hempelmann, *J. Mater. Res.*, 1998, **13**, 3174.
3 K. Osseo-Asare and F. J. Arriagada, *Ceram. Trans.*, 1990, **12**, 3.
4 J. A. Beunen and E. Ruckenstein, *Adv. Colloid Interface Sci.*, 1982, **16**, 201.
5 V. Pillai, P. Kumar and D. O. Shah, *Adv. Colloid Interface Sci.*, 1995, **55**, 241.
6 L. Qui, J. Ma, H. Cheng and Z. Zhao, *Colloids Surf.*, 1996, **108**, 117.
7 M. Roth and R. Hempelmann, *Chem. Mater.*, 1998, **10**, 78.
8 R. Hoppe, W. Liebe and W. Z. Dähne, *Z. Anorg. Allg. Chem.*, 1961, **307**, 276.
9 J. H. Payne, *J. Am. Chem. Soc.*, 1937, **59**, 947.
10 M. E. Straumanis, *Acta Crystallogr.*, 1949, **2**, 82.
11 R. J. Gehr and R. W. Boyd, *Chem. Mater.*, 1996, **8**, 1807.
12 A. Kitahara, *Proc. Int. Cong. Surf. Active Substances II*, Editiones Barcelone, 1968.
13 C. Petit, P. Lixon and M. P. Pileni, *J. Phys. Chem.*, 1990, **94**, 1598.
14 B. E. Warren and B. L. Averbach, *J. Appl. Phys.*, 1950, **21**, 595.
15 H. Natter, T. Krajewski and R. Hempelmann, *Ber. Bunsenges. Phys. Chem.*, 1996, **100**, 55.

16 J. Krill and B. Birringer, *Philos. Mag. A*, 1998, **77**, 621.
17 L. M. Mille, *An. Espana*, 1945, **41**, 120.
18 V. Chabra, V. Pillai and B. K. Mishra, *Langmuir*, 1995, **11**, 3307.
19 M. Dvolaitzky and R. Ober, *J. Dispersions Sci. Technol.*, 1983, **4**, 29.
20 C. F. Karayigitoglu, *Colloids Surf. A*, 1994, **82**, 151.
21 M. J. Hou and D. O. Shah, *Interfacial Phenomena in Biotechnology and Materials Processing*, ed. Y. A. Attia and S. Chander, Elsevier Science Publishers B.V., Amsterdam, 1988, p. 443.
22 J. B. Nagy, *Colloids Surf.*, 1989, **36**, 229.

Paper 8/07301E